Proceedings of the
15th IFAC Symposium on System Identification
Saint-Malo, France, July 6-8, 2009

Design, Modeling and Stabilization of a Moment Exchange Based Inverted Pendulum

Jordan Meyer, Nathan Delson and Raymond A. de Callafon

Dept. of Mechanical and Aerospace Engineering, University of California, San Diego, 9500 Gilman Drive 0411, La Jolla, CA 92093

Abstract: This paper summarizes the mechanical and control design concepts of an inverted or unstable pendulum where stabilization is achieved by a moment exchange generated by a controlled symmetric rotation of a rotational inertia attached to the pendulum. The proposed design of the pendulum has a fixed bottom rotation or point of support as opposed to the usual vertically or horizontally moving point of support to stabilize the pendulum, allowing for small form factor desktop design of an inverted pendulum experiment. The symmetry of the rotational inertia allows for stabilization of the pendulum without the need to control the position of the mass attached to the pendulum. The paper reviews the design considerations, dynamic modeling, system identification and control design strategy to stabilize the pendulum.

1. INTRODUCTION

For demonstration and evaluation of intricate concepts behind automatic control, the upside-down or inverted pendulum Acheson and Mullin (1993) has been an extensively used application in both research and teaching of control system design. The classical inverted pendulum as described for example in Landau and Lifshitz (1976) is constraint to move on a vertical plane and under the influence of a (destabilizing) gravity force, while the point of support can be subjected to horizontal or vertical forces. Stability studies using vertical oscillations of the point of support date back to Stephenson (1908), but the classical inverted pendulum still serves as a benchmark for many control algorithms Aracil and Gordillo (2004). The development of new (non)linear control design methodologies for the classical and more complex inverted pendulums is still an active research area, see e.g. Cheng et al. (2005); Xu and Yu (2004); Casavola et al. (2004); Lundberg and Roberge (2003); Alonso et al. (2002).

In most of the control algorithms for the stabilization of the classical inverted pendulum, horizontal forces on the point of support are provided by a cart mechanism. By the controlled movement of the cart, stabilization of a single or even multiple inverted pendulums can be achieved Shen et al. (2005). Unfortunately, horizontal movement of the point of support of the pendulum requires a relative large horizontal surface for the operating range of the inverted pendulum. In addition, either belt driven motors, linear actuators or a controllable cart is required to stabilize the pendulum.

The objective of this paper is to summarize the main design, modeling and identification concepts behind an inverted pendulum that can be stabilized via a moment exchange with a rotating inertia. Such a inverted pendulum design can be operated on a much smaller footprint and operates with a fixed rotational point of support. This paper also shows an optimization of moment exchange gear ratio to maximize the angle from which the pendulum can be brought to an upright position.

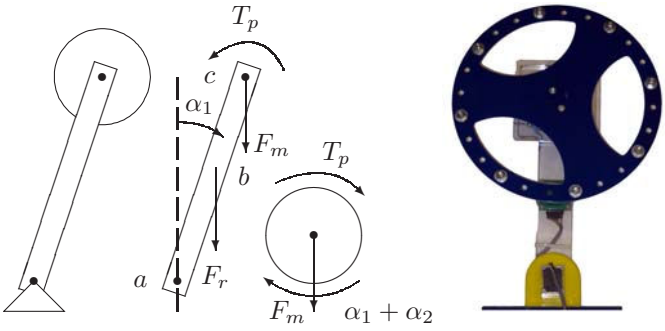

Fig. 1. Schematics (left) and actual device (right) of inverted pendulum with rotating inertia for moment exchange stabilization

To illustrate the main idea behind the moment exchange inverted pendulum, consider the (inverted) pendulum depicted in Figure 1. The pendulum consists of an inverted rod (pendulum) connected to a rotating inertia. By accelerating the rotating inertia, a moment exchange can be generated between the rod and the inertia. The moment exchange generates a moment that could be used to stabilize the inverted pendulum or dampen out the motion of a stable pendulum. Due to the moment exchange the pendulum does not need a moving base or cart for stabilization, allowing a much simpler table-top design.

2. PENDULUM DYNAMICS

2.1 Equations of motion

With the configuration depicted in Figure 1, the absolute angular rotation $\alpha_1(t)$ of the pendulum rod and the relative rotation $\alpha_2(t)$ of the rotating inertia can be described by

978-3-902661-47-0/09/$20.00 © 2009 IFAC 10.3182/20090706-3-FR-2004.0326

$$\begin{aligned} I_p^a \ddot{\alpha}_1(t) &= F_r l_b \sin\alpha_1(t) + F_m l_c \sin\alpha_1(t) - T_p(t) \\ I_m^c(\ddot{\alpha}_1(t) + \ddot{\alpha}_2(t)) &= T_p(t) \end{aligned} \quad (1)$$

In (1) the following variables are used: I_p^a indicates the angular momentum of the inverted pendulum around the bottom rotation point a. I_m^c indicates the angular momentum of the rotating inertia around its center and connection point c. F_r is the gravitational force due to the pendulum rod mass acting at the center of gravity at point b a distance l_b from point a along the pendulum. F_m is the is the gravitational force due to the rotating inertia located at point c a distance l_c from point a along the pendulum. $T_p(t)$ is a torque or moment exchange generated internally between the pendulum rod and the rotating inertia and will be used to stabilize the pendulum.

The symmetry of the rotating mass simplifies the equations of motion in a number of ways; the centrifugal forces all pass through the pendulum pivot point and therefore do not effect the dynamics of the system, there is no gravitational component dependent on α_2, and there are no Coriolis forces Asada and Slotine (1986). Physical properties such as length and diameter of the pendulum are mostly determined by design considerations. In order to obtain numerical values for the coefficients of the differential equation given in (1), we parametrize the coefficients in terms of the design parameters:

Definition 1. The physical design parameters of the inverted pendulum are characterized by the masses m_r, m_m, the dimensions l, r and R that are defined as follows:

- The total mass m_r and m_m of respectively the pendulum rod and the rotating inertia.
- The total length l and the width or radius r of the pendulum rod.
- The radius R of the cylindrical rotating inertia where R reflects the maximum value allowed by space constraints.

Gravitational forces and inertial constants can be expressed in terms of the above defined physical design parameters. The gravitational forces acting on the pendulum are given by

$$F_r = m_r g,\ F_m = m_m g,\ g = 9.81\text{m/s}^2$$

where m_r and m_m denote respectively the mass of the pendulum rod and the rotating inertia. In addition, the center of gravity located at distances l_b and l_c can be described by

$$l_b = \beta l,\ \beta \in (0,1),\ l_c = \gamma l,\ \gamma \in (0,1) \quad (2)$$

where l is the known length of the pendulum rod and the free parameters $0 < \beta, \gamma < 1$ model the center of gravity of the pendulum rod and the location of the pure moment generated by the rotating inertia. This definition rewrites the total gravity force contribution in (1) as

$$\begin{aligned} &F_r l_b \sin\alpha_1(t) + F_m l_c \sin\alpha_1(t) = \\ &m_p g l \sin\alpha_1(t),\ m_p = m_r\beta + m_m\gamma \end{aligned} \quad (3)$$

In case the mass of pendulum rod is evenly distributed, e.g. the pendulum rod is a perfect cylinder, then $\beta = 1/2$. In case the rotating inertia is mounted at the end of the pendulum rod then $\gamma = 1$.

The total moment of inertia I_p^a of the pendulum around the point a is the combined effect of the moment inertia of the pendulum rod I_r^a and the moment of inertia of the rotating inertia I_m^a with respect to point a. To write down analytic expressions for the moment of inertia we can use the parallel axis theorem

$$I_r^a = I_r^b + m_r(\beta l)^2 = I_r^b + \beta^2 m_r l^2$$

and assume a particular shape for the pendulum rod. The parameter $0 < \beta < 1$ is obtained from (2) and parametrizes the center of gravity of the pendulum rod. The moment of inertia I_r^b of the pendulum rod around the point b is given by $I_r^b = \frac{1}{12}m_r l^2 + \frac{1}{4}m_r r^2$ or $I_r^b = \frac{1}{12}m_r l^2 + \frac{1}{12}m_r r^2$ in case the pendulum rod with mass m_r and length l is respectively a homogeneous cylinder with a radius r or a homogeneous beam with a width r. For the different configurations of the pendulum rod, the expression of the inertia I_r^b of the pendulum rod around the point b can be generalized to

$$I_r^b = \mu m_r l^2 + \nu m_r r^2 \quad (4)$$

and in case the pendulum rod is not homogeneous, the parameters $0 < \mu, \nu < 1$ can also be used to model the inertial contributions respectively due to mass distribution, length and width dimension of the pendulum rod.

Using the parallel axis theorem, I_m^a of the rotating inertia with respect to point a can be written as

$$I_m^a = I_m^c + m_m(\gamma l)^2 = I_m^c + \gamma^2 m_m l^2$$

where the moment of inertia I_m^c around the (center) point c of the rotating inertia is given by

$$I_m^c = \frac{1}{2}m_m R^2$$

assuming a cylindrically shaped rotating inertia with mass m_m and radius R. The parameter $0 < \gamma < 1$ is again obtained from (2) and models the location of the rotating inertia along the pendulum rod.

It should be noted that m_m indicates the total mass of the rotating inertia, e.g. m_m would also include the mass of the rotor of a servo motor used to generate the moment exchange torque. With the addition of a servo motor, the assumption of a cylindrically shaped rotating inertia would not be viable. In that case, the moment of inertia of the rotating inertia with a radius R with respect to point c can be parametrized by

$$I_m^c = \tau m_m R^2 \quad (5)$$

where $0 < \tau < 1$ can be used to model any cylindrically shaped rotating inertia with outer radius R and possibly connected to a servo motor. Combining the results yields the total inertia of the inverted pendulum

$$I_p^a = I_r^a + I_m^a = (\beta^2 + \mu)m_r l^2 + \nu m_r r^2 + \gamma^2 m_m l^2 + \tau m_m R^2 \quad (6)$$

Combining the analytic expressions for the gravitational forces and inertial constants allows the differential equation in (1) to be written in the physical design parameters of the inverted pendulum. With (3), (5) and (6), the differential equation in (1) can be written as

$$\begin{aligned} I_p^a \ddot{\alpha}_1(t) &= m_p g l \sin\alpha_1(t) - T_p(t) \\ I_m^c \ddot{\alpha}_2(t) &= -I_m^c \ddot{\alpha}_1(t) + T_p(t) \\ I_p^a &= (\beta^2 + \mu)m_r l^2 + \nu m_r r^2 + \gamma^2 m_m l^2 + I_m^c \\ I_m^c &= \tau m_m R^2 \\ m_p &= m_r\beta + m_m\gamma \end{aligned} \text{, where} \quad (7)$$

2.2 Servo motor dynamics

A servo motor is used to create the internal torque $T_p(t)$ to stabilize via a moment exchange on the inverted pendulum. The torque created by a brushed DC motor can be described by

$$T_p(t) = K_m i_m(t)$$

where K_m is the motor constant and $i_m(t)$ is the current supplied to the DC motor. For a first order approximation, the dynamics of the servo motor due to a (small) inductance can be neglected. Using Ohm's law with a back EMF voltage proportional to the motor velocity $\dot{\alpha}_m(t)$, the motor current $i_m(t)$ satisfies

$$i_m(t) = \frac{V_m(t) - K_e \dot{\alpha}_m(t)}{R_m}$$

where $V_m(t)$ is voltage applied to the motor, K_e is the back EMF constant and R_m is the internal resistance of the motor. In case a gear box is used to increase the motor torque, the motor speed $\dot{\alpha}_m(t)$ is related to the angular speed $\dot{\alpha}_2(t)$ of the rotating inertia via

$$\dot{\alpha}_m(t) = \kappa \dot{\alpha}_2(t),\ \kappa > 1$$

creating a torque $T_p(t)$ that is given by

$$T_p(t) = \kappa \frac{K_m}{R_m} V_m(t) - \kappa^2 \frac{K_m}{R_m} K_e \dot{\alpha}_2(t) \tag{8}$$

Combining (7) with (8) yields the (non-linear) equations of motion of the inverted pendulum in explicit integration form

$$\begin{aligned} \ddot{\alpha}_1(t) &= \tfrac{1}{I_p^a} m_p g l \sin\alpha_1(t) + \tfrac{1}{I_p^a}\kappa^2 \tfrac{K_m}{R_m} K_e \dot{\alpha}_2(t) \\ &\quad - \tfrac{1}{I_p^a}\kappa \tfrac{K_m}{R_m} V_m(t) \\ \ddot{\alpha}_2(t) &= -\tfrac{1}{I_p^a} m_p g l \sin\alpha_1(t) - \tfrac{I_p^a + I_m^c}{I_p^a I_m^c}\kappa^2 \tfrac{K_m}{R_m} K_e \dot{\alpha}_2(t) \\ &\quad + \tfrac{I_p^a + I_m^c}{I_m^c I_p^a}\kappa \tfrac{K_m}{R_m} V_m(t) \end{aligned} \tag{9}$$

in which the motor voltage $V_m(t)$ is used as an input variable. The explicit integration form of (9) allows straightforward (non-linear) dynamic simulation of the ordinary differential equations using standard numerical methods, e.g. 4th order Runge-Kutta algorithm.

2.3 Linearized model of pendulum for control design

To simplify analysis and the design of a linear control algorithm, a linearized model of the inverted pendulum can be derived by assuming small perturbation of the pendulum angle $\alpha_1(t)$. Linearization around the upright position with $\alpha_1(t) = 0$, the equations of motion in (9) can be approximated by a set of coupled linear first order linear differential equations with $\sin\alpha_1(t) \approx \alpha_1(t)$. Since the position $\alpha_2(t)$ of the rotating inertia is not of importance during the control design, the state vector $x(t)$ is chosen to be

$$x(t) = [\ \alpha_1(t)\ \ \dot{\alpha}_1(t)\ \ \dot{\alpha}_2(t)\ ]^T \tag{10}$$

leading to a state space model

$$\dot{x}(t) = Ax(t) + BV_m(t)$$

in which all states could potentially be measured and

$$\begin{aligned} A &= \begin{bmatrix} 0 & 1 & 0 \\ \frac{1}{I_p^a} m_p g l & 0 & \frac{1}{I_p^a}\kappa^2 \frac{K_m}{R_m} K_e \\ -\frac{1}{I_p^a} m_p g l & 0 & -\frac{I_p^a + I_m^c}{I_p^a I_m^c}\kappa^2 \frac{K_m}{R_m} K_e \end{bmatrix}, \\ B &= \begin{bmatrix} 0 \\ -\frac{1}{I_p^a}\kappa \frac{K_m}{R_m} \\ \frac{I_p^a + I_m^c}{I_p^a I_m^c}\kappa \frac{K_m}{R_m} \end{bmatrix} \end{aligned} \tag{11}$$

Stability analysis of the state-space model in (11) is straightforward for an ideal DC-motor with a zero back EMF constant $V_e = 0$. In that case, the poles for $g > 0$ (inverted pendulum) lie at 0 and $\pm\sqrt{m_p g l / I_p^a}$ with m_p defined in (3), indicating the instability of the mechanical system. For $g < 0$ (stable pendulum) a marginally stable system is obtained with all poles on the imaginary axis. In case the back EMF constant $V_e \neq 0$, the shorthand notation

$$A = \begin{bmatrix} 0 & 1 & 0 \\ \theta_1 & 0 & \theta_2 \\ -\theta_1 & 0 & -\theta_3 \end{bmatrix} \tag{12}$$

for the state space matrix A with

$$\theta_1 = \frac{1}{I_p^a} m_p g l,\ \theta_2 = \frac{1}{I_p^a}\kappa^2 \frac{K_m}{R_m} K_e,\ \theta_3 = \frac{I_p^a + I_m^c}{I_p^a I_m^c}\kappa^2 \frac{K_m}{R_m} K_e$$

indicates that

$$\det(\lambda I - A) = \lambda^3 + \theta_3 \lambda^2 - \theta_1 \lambda - \theta_1(\theta_3 - \theta_2)$$

Since $\theta_3 > \theta_2 > 0$, a standard Routh-Hurwitz criterion indicates that A is Hurwitz provided $\theta_1 < 0$, requiring $g < 0$ (stable pendulum). In addition, if $g > 0$ (inverted pendulum), the Routh-Hurwitz procedure indicates the presence of a single right half plane pole.

3. DESIGN CONSIDERATIONS FOR INVERTED PENDULUM

3.1 Design constraints

As indicated in Definition 1, the physical design parameters reflect the length l and the width/radius r of the pendulum rod, the mass m_r of the pendulum rod, the mass m_m of the rotating inertia, and the radius R of the rotating inertia. The generalized mass m_p of the inverted system, the inertia I_p^a of the inverted pendulum around the bottom rotation point a and the inertia I_m^c of the rotating inertia around its rotation point c are all combinations of the physical design parameters m_r, m_m, l, r and R. The combinations are weighted by the parameters

- $0 < \beta < 1$ defined in (2) and parametrizes the center of gravity of the pendulum rod. In case the mass of pendulum rod is evenly distributed, then β is restricted to $\beta = 1/2$.
- $0 < \gamma < 1$ defined in (2) and parametrizes the location of the rotation point c along the pendulum rod. In case the rotating inertia is mounted at the end of the pendulum rod then γ is restricted to $\gamma = 1$.
- $0 < \mu < 1$ defined in (4) and parametrizes the inertial constant due to the length of the pendulum rod. If the pendulum rod is chosen to homogeneous, then μ is restricted to $\mu = 1/12$, but can be made smaller by a non-homogeneous design.
- $0 < \nu < 1$ defined in (4) and parametrizes the inertial constant due to the radius or with r of the pendulum

rod. If the pendulum rod is a homogeneous cylinder with radius r, then $\nu = 1/4$. If the pendulum rod is a homogeneous beam with a width r, then $\nu = 1/12$.

- $0 < \tau < 1$ defined in (5) and parametrizes the inertial constant of the circular rotational inertia. If the rotational inertia is cylindrically shaped, then $\tau = 1/2$. However, τ can be made larger than $1/2$ by distributing the mass along the outside of the maximum radius R of the rotating inertia.

Given the design constraints imposed by the physical design parameters m_r, m_m, l, r, R of the pendulum, optimization of the pendulum design can be done by lowering the contribution of the (destabilizing) gravitational forces and increasing the effect of the (stabilizing) moment exchange. With

$$I_p^a = I_r^a + I_m^a = I_r^a + I_m^c + \gamma^2 m_m l^2 \tag{13}$$

we see from (7) for $\alpha_1(t) = 0$ (upright position of pendulum) that

$$\frac{\ddot{\alpha}_1(t)}{\ddot{\alpha}_2(t)} = -\frac{I_m^c}{I_p^a + I_m^c} = -\frac{\tau m_m R^2}{I_r^a + (2\tau R^2 + \gamma^2 l^2) m_m}$$

Given a length l of the pendulum rod and a maximum diameter R of the rotating inertia located at point c at $l_c = \gamma l$ along the pendulum rod, maximum moment exchange can be obtained by maximizing both the inertial constant τ and the mass m_m of the rotating inertia. However, a larger value of m_m increases the contribution of the (destabilizing) gravitational force. This causes the unstable pole at $\sqrt{m_p g l / I_p^a}$ with m_p defined in (3) to move further into the right half plane and requiring larger control signals (moment exchange) to stabilize the pendulum.

3.2 Optimizing gear box ratio

The trade off between the choice of the mass m_m of the rotating inertia and the the required moment exchange for stabilization of the pendulum can be addressed by the proper choice of the gear ratio κ. In addition, the gear ratio κ plays an important role in the familiar (linear) torque-speed curve that models the relationship between angular velocity $\dot{\alpha}_2(t)$ and motor torque $T_p(t)$. Allowing maximum voltage $V_m(t) = V_m^{max}$ $\forall t$ to be applied to the motor, a linearly declining torque-speed curve is obtained with a stall torque T_p^{max} at $\dot{\alpha}_2(t) = 0$ and maximum angular speed $\dot{\alpha}_2^{max}$ at $T_p(t) = 0$ given by

$$T_p^{max} = \kappa \frac{K_m}{R_m} V_m^{max}, \;\; \dot{\alpha}_2^{max} = \frac{1}{\kappa K_e} V_m^{max}$$

Although the gear box ratio κ increases the internal torque (stall) $T_p(t)$, it comes with a price of a sharper decline of the motor-speed curve and a smaller velocity range of the rotating inertia.

For the purposes of selection of the optimal gear ratio κ, frictional losses in the gear are neglected. To optimize the value κ for different values of the mass m_m, we propose to maximize the operating range of the inverted pendulum. The initial-state stabilizing operating range is defined as the maximum initial angle $|\alpha_1(t)| \neq 0$ at $t = 0$ for which inverted pendulum can be brought back to $\alpha_1(t) = 0$ (upright position) for some $t > 0$ by applying a maximum voltage $V_m(t) = V_{max}$ to the DC-motor. To determine the initial operating range, a grid of (initial) values of the mass m_m and the gear box ration κ is used to compute $\alpha_1(t)$ for $V_m(t) = V_{max}$ using the non-linear model in (9). Minimization of

$$\min_{\alpha_1(0)} \alpha_1^2(t)$$

at each (m_m, κ) grid point using a scalar bounded nonlinear function minimization such as `fminbnd` implemented in Matlab™ will find a maximum initial value $|\alpha_1(0)| \neq 0$ for which $\alpha_1(t) = 0$ (upright position). The results have been depicted in Figure 2 where it can be seen that an optimal gear ratio κ can be computed for any value of m_m to maximize the initial angle $\alpha_1(0)$ for which the pendulum can be stabilized.

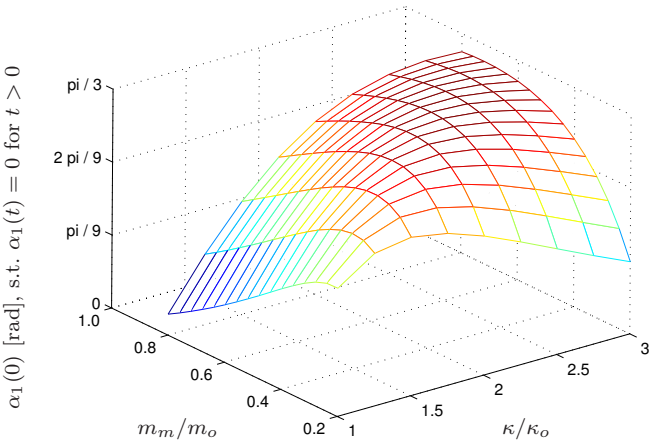

Fig. 2. Maximum initial angle $\alpha_1(0)$ for which $\exists t > 0$ with $\alpha_1(t) = 0$ as a function of a normalized mass m_m/m_o and normalized gear ratio κ/κ_o

4. IDENTIFICATION OF PENDULUM DYNAMICS

4.1 Parametrization of model

In order to complete the development of a dynamical model of the pendulum for control design, system identification techniques can be used to estimate accurate numerical values of the state space model in (11). Using measurements of the state variables $x(t)$ as defined in (10), the unknown coefficients in (11) can be written as

$$\begin{bmatrix} \ddot{\alpha}_1(t) \\ \ddot{\alpha}_2(t) \end{bmatrix} = \theta_1 \begin{bmatrix} 1 \\ -1 \end{bmatrix} \alpha_1(t) + \begin{bmatrix} \theta_2 \\ \theta_3 \end{bmatrix} \dot{\alpha}_2(t) + \begin{bmatrix} \theta_4 \\ \theta_5 \end{bmatrix} V_m(t) \tag{14}$$

where the additional parameters θ_4 and θ_5 are used to model the scaling gains for the map from the input to the state.

It can be noted here that a canonical observable parametrization of a third order state space model allows a six dimensional parameter for estimation purposes Ljung (1999). The reduction from six to five parameters is due to the knowledge of the state space model based on the analytic modeling of the pendulum in (11) allowing a grey-box based modeling approach Huang and Huang (2000). The linear parametrization given in (14) can be written into linear regression form

$$Y(k\Delta T) = \Theta X(k\Delta T) + E(k\Delta T), \;\; \Theta = [\, \theta_1 \; \cdots \; \theta_5 \,] \tag{15}$$

where the error $E(k\Delta T)$ is used to model the effects of noise on the measured state vector $x(t)$ in (10) and construction of the derivatives via (16). Assuming the collection of N data points, a standard Least-Squares solution

$$\Theta = \sum_{k=1}^{N} Y(k\Delta T)X^T(k\Delta T)\left[\sum_{k=1}^{N} X(k\Delta T)X^T(k\Delta T)\right]^{-1}$$

can be used to minimize the least-square error of $E(k\Delta T)$ and yields the parameter estimate for the state space model in (11).

4.2 Experiment design and results

In order to estimate the parameters of the pendulum over a significant number N of data points, experiments can be conducted on a stable pendulum ($g < 0$), allowing standard open-loop identification techniques. Estimation of the parameters Θ of the stable pendulum can easily be converted to the parameters of the unstable pendulum by $\Theta = [-\theta_1 \ \cdots \ \theta_5]$, as only the value of the gravitational acceleration constant g changes sign.

The derivative of the state vector can be approximated by

$$\ddot{\alpha}_i(k\Delta T) = \frac{\dot{\alpha}_i((k+1)\Delta T) - \dot{\alpha}_i(k\Delta T)}{\Delta T}, \ i = 1, 2 \quad (16)$$

based on discrete-time samples of the angular velocity $\dot{\alpha}_1(t)$ of the pendulum rod and the angular velocity $\dot{\alpha}_2(t)$ of the rotating inertia gathered at a sampling time ΔT. Measurement of $\dot{\alpha}_1(t)$ is possible by using an angular rate gyro attached to the pendulum rod, whereas $\dot{\alpha}_2(t)$ can be measured via an optical encoder on the DC servo motor.

θ_1	-39.3317
θ_2	0.3634
θ_3	0.3921

Table 1. Numerical values of parameters in state matrix A in (12) for the stable pendulum

Using a swept sine excitation running from 0.5 Hz till 5 Hz, experimental data of the angular position $\alpha_1(t)$ and the angular velocity $\dot{\alpha}_1(t)$ of the pendulum rod and relative rotation velocity $\dot{\alpha}_2(t)$ of the rotating inertia sampled at 25Hz are used to set up the linear regression problem in (15). Least squares estimation of the parameters yields the estimate given in Table 1 and a comparison between measured and the linear simulation of the states of the pendulum is depicted in Figure 3. The parameters in Table 1 give rise to the pole locations

$$-0.0287, \ -0.1817 \pm 6.2680j$$

for the stable pendulum. Changing sign on the parameter θ_1 gives the state matrix A for the inverted pendulum with pole locations

$$-0.0287, \ -6.4567, \ 6.0933$$

confirming the instability of the pendulum dynamics.

5. STABILIZATION OF PENDULUM VIA STATE FEEDBACK

5.1 Linear Quadratic Regulator Design

With the measurements of the states $\alpha_1(t)$, $\dot{\alpha}_1(t)$ and $\dot{\alpha}_2(t)$ of the inverted pendulum available for feedback,

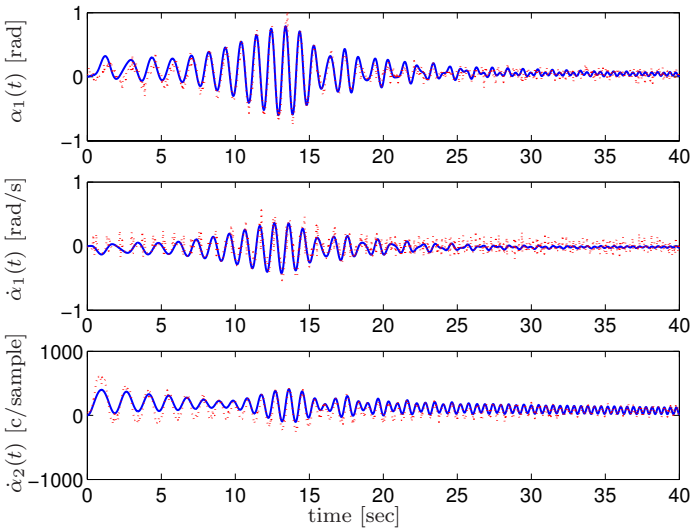

Fig. 3. Comparison between measured (dotted) and simulated (solid) angular pendulum position $\alpha_1(t)$ (top), angular pendulum velocity $\dot{\alpha}_1(t)$ and velocity $\dot{\alpha}_2(t)$ of rotational inertia

stabilization around the operating range of $\alpha_1(t) \approx 0$ rad can be done by a linear state feedback design, similar as e.g. Dan et al. (2004). A state feedback control law K with

$$V_m(t) = -Kx(t) = -K\left[\,\alpha_1(t) \ \dot{\alpha}_1(t) \ \dot{\alpha}_2(t)\,\right]^T$$

such that closed-loop system matrix $A - BK$ is Hurwitz can be computed using standard pole placement or optimal Linear Quadratic Regulator (LQR) techniques. In LQR a state feedback K is computed such that

$$\int_{-\infty}^{\infty} x^T(t)Qx(t) + V_m^2(t)dt, \ \dot{x}(t) = Ax(t) + BV_m(t)$$

is being minimized. The advantage of using LQR is the possibility to compute the minimal control energy solution by choosing $Q = 0$, creating a closed-loop system matrix $A-BK$ for which only the unstable eigenvalues of the state matrix A are mirrored into the left half plane Anderson and Moore (1971).

Choosing $Q > 0$ allows additional freedom in designing an optimal state feedback K. To provide additional design freedom we used the design concepts of LQR applied to a shifted state matrix $A + \epsilon I$:

$$\int_{-\infty}^{\infty} x^T(t)Qx(t) + V_m^2(t)dt, \ \dot{x}(t) = [A + \epsilon I]x(t) + BV_m(t)$$

to ensure that the eigenvalues $\lambda(A - BK)$ of the closed-loop matrix $A - BK$ satisfy $\mathrm{Re}\{\lambda(A - BK)\} < -\epsilon$.

5.2 Experimental results

With the choice of $Q = diag(10, 0, 100)$ and $\epsilon = 0.4$ a weighting is placed on the angular position $\alpha_1(t)$ of the pendulum and the angular velocity of the $\dot{\alpha}_2(t)$ of the rotating inertia. The result of the LQR optimization is a state feedback

$$K = [-14.5620 \ 87.2084 \ -1.9137]$$

that places the closed-loop poles $\lambda(A - BK)$ at

$$-11.4846, \ -3.2086 \pm 3.1701j$$

and allowing the pendulum to settle within one second.

Control experiments were conducted at the System Identification and Control Laboratory (SICL) at the department of Mechanical and Aerospace Engineering at UCSD. The state feedback controller is implemented via a MicroChip™ PIC16F877A (Perhipheral Interface Controller). The PIC is programmed to use (only) a 10 bit AD conversion of the analog measurements of both the angular position $\alpha_1(t)$ of the inverted pendulum obtained via a Memsic™ mxa2500GL accelerometer and the angular velocity $\dot{\alpha}_1(t)$ obtained via a Analog Devices™ adxrs300 angular rate gyro. In addition, the PIC is interfaced to an LSI/CSI™ LS7166 24 bit quadrature counter to measure the optical encoder output attached to the DC-motor to compute an estimate of the DC motor velocity $\dot{\alpha}_2(t)$ via a discrete-time derivative. Data sampling is done at 100Hz, whereas a hardware coded on-chip 10bit PWM (Pulse Width Modulation) at 19.5kHz and a digital output for direction on the PIC is used to control the DC-motor via a bidirectional H-bridge circuit. Signals are routed to a National Instruments™ PXI system for real-time prototyping and monitor the performance of the control system.

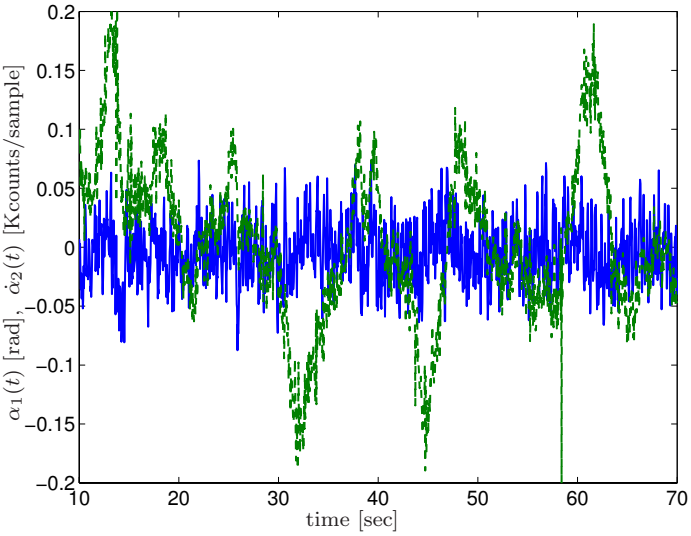

Fig. 4. Time traces of angular pendulum position $\alpha_1(t)$ (solid) and and velocity $\dot{\alpha}_2(t)$ of rotational inertia (dotted) during state-feedback control of inverted pendulum

A plot of the observed angular position $\alpha_1(t)$ and the motor velocity $\dot{\alpha}_2(t)$ is depicted in Figure 4. It can be observed that the inverted pendulum stays within ± 0.05 rad $\approx \pm 3$ deg while keeping the velocity of the rotating inertia in the range of 200 counts/sample.

6. CONCLUSIONS

The dynamical model of the inverted pendulum with a moment exchange wheel can been written explicitly in terms of the design parameters that include length, width and mass of pendulum rod and mass and diameter of the rotating inertia. To address the design trade-off between motor speed and delivered motor torque for moment exchange, a method to optimize the gear ratio and mass of the rotating inertia has been proposed.

Both a non-linear and linearized model of the pendulum can be derived by Newtonian mechanics and the linear model is easily written in a third order state space representation with an explicit (grey-box) parameterization of the unknown model parameters. A Least-Squares estimation technique for estimation of the model parameters is proposed showing excellent agreement between measured and simulated data. The paper also illustrates the successful implementation of a (real-time embedded) state feedback control law to stabilize the pendulum.

REFERENCES

D.J. Acheson and T. Mullin. Upside-down pendulums. *Nature*, 366:215–216, 1993.

D.M. Alonso, E.E. Paolini, and J.L. Moiola. Controlling an inverted pendulum with bounded controls. *Dynamics, Bifurcations, and Control (Lecture Notes in Control and Information Sciences)*, 273:3–16, 2002.

B.D.O. Anderson and J.B. Moore. *Linear Optimal Control*. Prentice-Hall, Englewood Cliffs, New Jersey, USA, 1971.

J. Aracil and F. Gordillo. The inverted pendulum: A benchmark in nonlinear control. In *Proc. Of the World Automation Congress*, pages 468–482, Piscataway, NJ, USA, 2004. IEEE.

H. Asada and J.-J. E. Slotine. *Robot Analysis and Control*. John Wiley & Sons, New York, NY, USA, 1986.

A. Casavola, E. Mosca, and M. Papini. Control under constraints: An application of the command governor approach to an inverted pendulum. *IEEE Transactions on Control Systems Technology*, 12:193–204, 2004.

Luo Cheng, Hu De-Wen, Zhu Xiao-Cai, and Dong Guo-Hua. Quintuple inverted pendulum control based on LQR and fuzzy piecewise interpolation. *Kongzhi Yu Juece/Control and Decision*, 20:392–397, 2005.

Huang Dan, Zhou Shaowu, Wu Xinkai, and Zhang Zhifei. An inverted pendulum based on the LQR optimal regulator. *Control and Automation*, 2:37–38, 2004.

Shiuh-Jer Huang and Chien-Lo Huang. Control of an inverted pendulum using grey prediction model. *IEEE Transactions on Industry Applications*, 36:452–458, 2000.

L.D. Landau and E.M. Lifshitz. *Mechanics, 3d Edition*. Pergamon Press, Oxford, 1976.

L. Ljung. *System Identification: Theory for the User (Second Edition)*. Prentice-Hall, Englewood Cliffs, New Jersey, USA, 1999.

K.H. Lundberg and J.K. Roberge. Classical dual-inverted-pendulum control. In *Proc. 42nd IEEE International Conference on Decision and Control*, pages 4399–4404, Piscataway, NJ, USA, 2003. IEEE.

B.H. Shen, G.L. Hsu, M.C. Tsai, M.F. Hsieh, M.C. Wu, and C.R. Chiang. Synchronous control of the parallel dual inverted pendulum system driven by linear servomotors. In *Proc. IEEE International Conference on Mechatronics*, pages 157–161, Piscataway, NJ, USA, 2005. IEEE.

A. Stephenson. On a new type of dynamical stability. *Mem. Proc. Manch. Lit. Phil. Soc.*, 52:1–10, 1908.

Chao Xu and Xin Yu. Mathematical modeling of elastic inverted pendulum control system. *Journal of Control Theory and Applications*, 2:281–282, 2004.